省リソース型不要ガス除去手法の検討

○大西 充，島 明日香，小口美津夫，桜井誠人(宇宙航空研究開発機構)，奥谷 猛(横浜国立大学)

Study on a Low-Resource Removal Method for Useless Gases

Mitsuru OHNISHI, Asuka SHIMA, Mitsuo OGUCHI, Masato SAKURAI (JAXA), Takeshi OKUTANI
(Yokohama National Univ.)

1. Introduction

In order to establish a low-resource air-revitalization system as a simplified ECLSS, a new material called "**M**ulti-**F**unctional **A**ctivated **C**arbon" which consists of zeolite and activated carbon is being developed. The material has a potential to remove not only CO_2 and water vapor but also harmful gases from the air simultaneously. In this paper, the material on CO_2 adsorption and a newly developed numerical simulation program for extrapolation of experimental results of adsorption using MFAC are briefly introduced.

2. Multi-Functional Activated Carbon

Rice husk as raw material of MFAC has following features.

1) Dried Rice husk has 20% of SiO_2.
2) Baked husk consists of 50% SiO_2 and 50% Carbon.
3) Zeolite can be made from SiO_2.
4) Nano-level combined Zeolite+Carbon can be made.

From the above features, MFAC's expected features as adsorbent are as follows.

1) Zeolite is an adsorbent for CO_2.
2) Zeolite is a strong adsorbent for H_2O
3) Carbon can make H_2O adsorption moderate.
4) Activated carbon is an adsorbent for harmful gasses.
5) MFAC can simultaneously adsorb CO_2, H_2O and harmful gasses.

The current status of MFAC development is as follows.

1) 1cc of MAFC have been successfully produced.
2) 10cc-class MFAC production was failed. The production process of MFAC should be improved.
3) Pelletization of MFAC seems to be successful.

3. Numerical Simulation

Many adsorption tests for several adsorbents were made. These results show a simple model as shown in **Fig.1(a)** can't explain their adsorption processes and experimental approaches to understand the adsorption phenomena has limitations. Therefore, a numerical method with diffusion coefficient as shown in **Fig. 1(b)** is being introduced. The comparison of experimental result using MS-5A (a kind of zeolite) and numerical simulation one for CO_2 adsorption is shown in **Fig. 2**. The simulation result agrees very well with the experimental one.

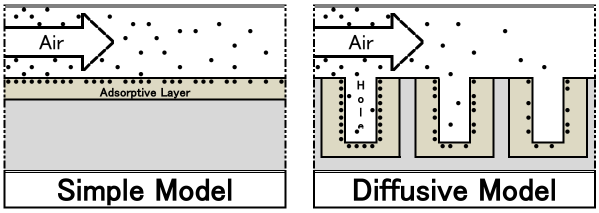

(a) (b)

Fig. 1 Simple model and diffusive model

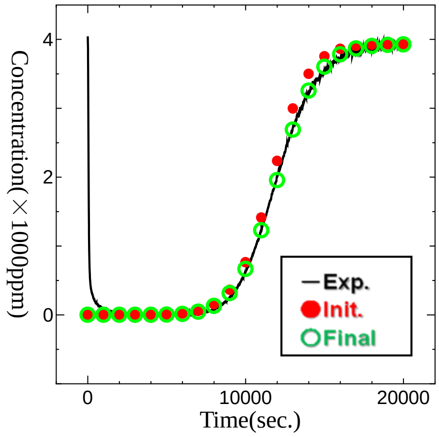

Fig. 2 Experimental result and numerical simulation one of CO_2 adsorption

4. Summary

The development of MFAC is partially achieved. The new numerical simulation program with the diffusive model for adsorption processes is successfully developed.

References

1) M. Ohnishi, A. Shima, M. Oguchi, M. Sakurai and T. Okutani: Proc. of 54th Space Sciences and Technology Conference, JSASS-2010-4297, 2010.

2) M. Ohnishi, A. Shima, M. Oguchi, M. Sakurai and T. Okutani: Proc. of 2011 SEE Conference, 2011, p17.

28A02

籾殻からの炭酸ガス– 水同時吸着材の開発

○奥谷　猛，水戸賢吾，内海友美（横国大），大西　充（JAXA）

Development of Simultaneous Absorbent for CO_2-$H_2$0 from Rice Hulls

Takeshi OKUTANI, Kengo MITO , Tomomi UTUMI (Yokohama National University),
Mitsuru OHNISHI (JAXA)

1. Introduction

When human stays in enclosed space such as space suit and space station, the gases such as CO_2 and H_2O discharged by human activities should be removed or reused or changed harmlessly. The absorbents such as Zeolites and activated carbon are not able to absorb CO_2 and H_2O simultaneously because of polarity. The absorbents used in circumstances necessary volume- and weight-saving such as space should absorb CO_2 and H_2O simultaneously.

To develop the absorbent for CO_2-H_2O mixture gas, the conjunctive activated carbon - zeolite composites were synthesized by hydrothermal reaction added Al_2O_3-NaOH-H_2O to the pyrolyzed rice hulls produced by thermal treatment in Ar at the temperature from 500 to 1000˚C. The molecule structures of the conjunctive composites were LTA, FAU or amorphous according to the pyrolyzed temperature of rice hulls. The absorption capacity of CO_2 for the conjunctive composites was higher than that for the mixture of activated carbon and 4A zeolite having the same specific surface area and Si/Al atomic ratio as those of the conjunctive composites.

2. Experimental

PRH500(PRH: Pyrolyzed Rice Hulls) was prepared to heat raw rice hulls to 500˚C by 5K/min in flowing N_2 of 100mL/min and to keep for 1hr. The activated carbon – Zeolite was produced by hydrothermal reaction of the PRH500 with NaOH, $Al(OH)_3$ and H_2O (Na_2O: Al_2O_3: SiO_2(contained in PRH500): H_2O=3.12:1:1.93:128) added commercial zeolite A as a seed of 1wt% for SiO_2 in the sample. The hydrothermal reaction was carried out using autoclave at 100˚C for 4hr with 100rpm. The hydrothermal products were filtered and dried to obtain the conjunctive activated carbon-zeolite composites (A_PRH500). Compared the reactivity of SiO_2 in rice hulls with that of α -quartz, the activated carbon-zeolite composites were prepared from α -quartz in the same process as that using rice hulls (A_quartz). To examine the effect of functional groups on the composites on the absorption of polar substance such as H_2O, theree samples were prepared; A_PRH500 was treated in N_2 at 500˚C for 3 hr (N_2_180), A_PRH500 was stirred in 10molH2O2 solution for 24 he at room temperature, and A_PRH500 was stirred in K_2CO_3 solutions (5wt%, 10wt% and 30wt% K_2CO_3) and dried.

The absorption experiments of CO_2-H_2O were carried out with flow-reactor combined with gas chromatograph in the Ar flowing containing 4000ppm CO_2-13~16mg/m^3 H_2O at 25˚C.

3. Results and Discussion

XRD patterns of A_PRH500, PRH500 and A_quartz are depicted in **Fig.1**. The crystalline structures of PRH500, A_PRH500 and A_quartz were amorphous, Linde type A zeolite (LTA) and α -quartz. A_quartz did not change to zeolite by the same hydrothermal reaction as that for PRH500. The rice hull silica has higher reactivity than α -quartz.

CO_2 can be absorbed on the surface of the absorbent, A_PRH500, which was removed acid functional group such as –OH and –COOH by heat treatment of A_PRH500 in N_2 at 500˚C. A_PRH500 treated by H_2O_2 solution to increase acid functional group on the surface of absorbent absorbed H_2O firmly and no CO_2. Acid functional group on the surface of absorbent absorbed H_2O with strong dipole moment. The A_PRH500 supported basic $CaCO_3$ absorbed CO_2 and the CO_2 concentration of 4000ppm reduced to 3000ppm as shown in **Fig.2**.

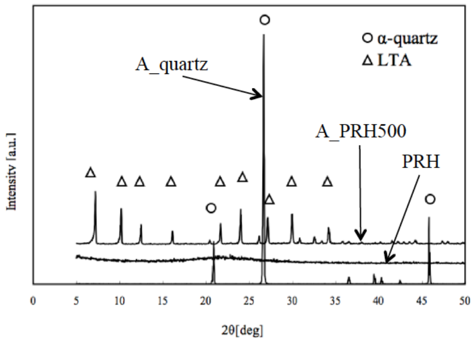

Fig.1. XRD pattern of A_PRH500, PRH and A_quartz.

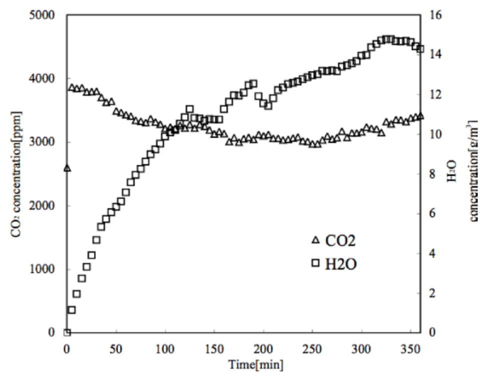

Fig.2. K_2CO_3 30wt% adsorption breakthrough curve.

28A03

ISS 以後の有人宇宙探査ミッションと生命維持技術

○桜井誠人、島明日香、曽根理嗣、小口美津夫、大西充（JAXA)

The Manned Space Exploration of the post ISS and Life Support Sytem

○Masato SAKURAI, Asuka SHIMA, Yoshitsugu SONE, Mitsuo OGUCHI, Mitsuru OHNISHI (JAXA)

1. Introduction

"JAXA road map", enacted in 2010 December (5th edition), defines development of a spacesuit, manned space ship, manned rover and manned lunar surface from the year 2020. The common and crucial key technology in these manned systems is ECLSS (Environmental Control and Life Support System), where air revitalization technology and water reclamation technology were both not achieved during development of (JEM) the Japanese Experiment Module. It is proposed that these technologies should be focused, to take initiative on promoting a manned based system.

The road map mentioned above also indicates the principles of utilizing ISS/JEM as an experimental proven test bed to leverage space technology effectively. Fluid, from an ECLSS technology prospective is an applied and promising technical demonstration item in a non-gravity ISS environment. An on-orbit Air Re-vitalization system and Water Reclamation system will be prepared by 2015 to commence technical demonstration on the ISS/JEM.

2. Field test for nest exploration of the post ISS

The next manned space mission of post ISS has been discussed. The field tests of simulation on future manned lunar or meteoroid space mission D-RATS (Desert Research and Technologies Simulations) are carried out in Flagstaff in Arizona State every September. LER (Lunar Electric Rover) and ATHLETE (All-Terrain Hex-Limbed Extra- Terrestrial Explorer) and so on are tested in outdoor.

From three years ago, HDU: the Habitation Demonstration Unit was appeared on the field test, ECLSS (Environmental Control and Life Support System) research started to the new stage. **Fig. 1** show D-RATS, the entrance, habitation module with inflatable structure in second floor, Hygiene Module, LER are shown in the figure. Remote operation of vehicles systems, evaluation of inflatable loft, etc was evaluated in D-RATS 2011.

3. ECLSS demonstration

In order to reduce the mass needing to be resupplied and disposed of, regenerative life support functions include oxygen recovery from carbon dioxide via the combination of CO_2 reduction via a Sabatier process and O_2 generative via an electrolysis process are studied. As ISS operation is extended to 2015-2020, ECLSS flight demonstration is planning on ISS.

A photograph of the water electrolysis system is shown in **Fig.2**. The test section is sized for installation in the JEM Multi-purpose Small Payload Rack (600 mm × 600 mm × 900 mm). The test result of the cathode feed water electrolyzer is shown in **Fig. 3**. The electrolysis voltage reduces with increasing temperature, giving a clear performance benefit of operating at higher temperature.

A technical issue is that gas-liquid separation is fundamentally different in a microgravity environment to behavior in a gravity field. It is assumed that the knowledge of fluid dynamics under microgravity will be applied for life support system[1)].

Fig.1 (left) HDU-DSH, the entrance, habitation module with inflatable structure in second floor, Hygiene Module, LER (from left to right)
Fig.2 (right) water electrolysis system

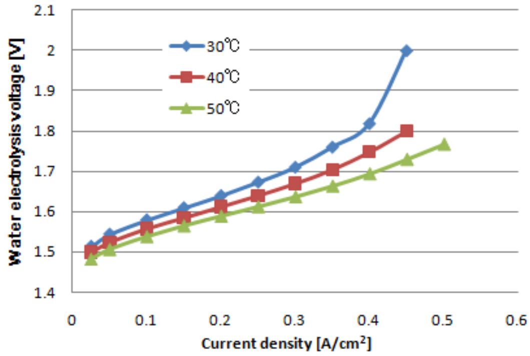

Fig. 3 result of water electrolysis I-V curve (Cathode feed)

4. Conclusion

Among ECLSS technologies, JAXA is approaching to prepare an on-orbit demonstration concerning air revitalization system around 2015.

References

1) Masato Sakurai, J. Jpn. Soc. Microgravity Appl. Vol.26 No.4, A103, 345 (2009)

28A04

JAXA における有人宇宙機用有害ガス処理装置の研究状況

○立原悟，佐藤直樹，大西充，桜井誠人（宇宙航空研究開発機構)

Status of Study of the Trace Gas Contaminant Remover for the Human Space Transportation System in JAXA

Satoru TACHIHARA, Naoki SATOH, Mitsuru OHNISHI, Masato SAKURAI (JAXA)

1. Introduction

In March 2005, the Japan Aerospace Exploration Agency (JAXA) announced the JAXA Vision, and formed an internal working group for Environment Control and Life Support (ECLS) systems to prepare for future human space missions.

This paper shows the results of a study of the CO_2/TGC Remover for the Human Space Transportation System (HSTS) that was performed in 2010 by the ECLS working group.

2. Status of Study of the CO_2/TGC Remove for the HSTS

2.1 Study Condition

(1) Target Mission

Mission of transporting crew to the International Space Station (ISS) was selected as the target, for the following reasons; 1)At present, a planetary exploration mission is not realistic for JAXA, 2)It seems a replacement crew transfer vehicle is needed following the retirement of the space shuttle, 3)Crew transfer to the ISS is the best mission for JAXA to verify the first HSTS.

(2) Trace Gas Contaminant (TGC) Load Model Development

After selection of the target, a TGC load model database consisting of 220 gases was developed based on the data, which were obtained through the development of Japanese module for the ISS. Subsequently, 16 gases that reached the "7 day Spacecraft Maximum Allowable Concentration (SMAC[1])" within the mission period were selected from the TGC load model database as a TGC load model for HSTS.

2.2. Concept Study

The working group studied the type of CO_2/TGC Remover, which is necessary for the HSTS of the 3 crew members/5 day mission. A regenerative CO_2 remover was selected, because a non-regenerative type would require a large mass exceeding 30kg to absorb 15kg of CO_2 generated from crew members. On the other hand, regenerative TGC remover was deemed not necessary, because of the short mission period.

Fig. 1 shows the result of a concept study of the CO_2/TGC Remover include Temperature and Humidity Controller (THC) for HSTS. The CO_2/TGC remover is located downstream of the THC to supply dried and cooled air to the CO_2/TGC remover. This location was selected, because the capability of the absorbent used in the TGC and CO_2 remover will be enhanced under dry and low temperature conditions. There are two CO_2 remover canisters, which can be operated alternately. When one CO_2 remover canister absorbs CO_2, another will be regenerated.

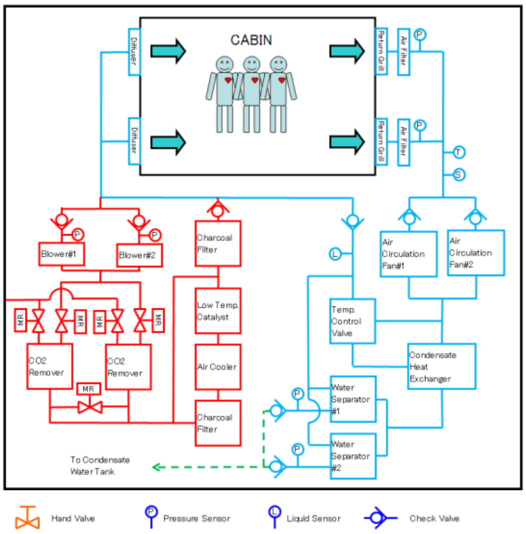

Fig. 1 Result of the concept study of the CO_2/TGC Remover.

2.3. Demonstration Test Results of the CO_2/TGC Remover

The working group performed a demonstration test of the CO_2/TGS remover for HSTS using absorbents and catalyst which has been studied by the working group[2] in parallel with the concept study. From the test results, the working group could confirm; 1)Methanol, Acetaldehyde, Acetone, Dichloro-benzene, and ammonia can removed by iodic acid-impregnated activated carbon, 2)Carbonyl Sulfide can removed by potassium hydroxide-impregnated activated carbon, 3)Methane and Carbon Monoxide can be completely oxidized to CO_2 at 350 degrees C by an oxidizer, 4)CO_2 can be removed by the JAXA CO_2 absorbent.

3. Conclusion

As shown in paragraphs 2, the JAXA ECLS systems working group studied the concept of a CO_2/TGC Remover for HSTS, and performed a demonstration test in 2010. In 2011, the working group will perform the further studies or tests to obtain design data and improve the design of the CO_2/TGC Remover.

References

1) NASA: SPACECRAFT MAXIMUM ALLOWABLE CONCENTRATIONS FOR AIRBORNE CONTAMINANTS, JSC-20584

2) Tachihara, S., Satoh, N., Ohnishi, M., Sakurai, M.,: Study Status of the ECLSS for the Next Manned Space Mission in JAXA, AIAA ICES 2010.

「きぼう」での FACET 実験 (1)

〇稲富裕光 (JAXA)，芦田幹大 (横浜国立大学)，阪田薫穂，吉崎泉 (JAXA)，島岡太郎 (JSF)，
曽根武彦 (JAMSS)，友部俊之 (IA)，奥谷猛 (横浜国立大学)，依田眞一 (JAXA)

FACET Experiment on "Kibo" (1)

〇Yuko INATOMI (JAXA), Motohiro ASHIDA (Yokohama National Univ.),
Kaoruho SAKATA, Izumi YOSHIZAKI (JAXA), Taro SHIMAOKA (JSF), Takehiko SONE (JAMSS),
Toshiyuki TOMOBE (IA), Takeshi OKUTANI (Yokohama National Univ.), Shinichi YODA (JAXA)

1. Introduction

The faceted cellular array growth represented by a sawtooth interface is often observed in zone-melting recrystallization of thin-film silicon single crystals and bulk oxide superconductor. Since this morphological development of the interface causes segregation of dopants, great interest in understanding the pattern formation in faceted cellular array growth has been taken over 30 years[1),2)]. Although many theoretical models have been proposed, there have been few works that experimental evidences are consistent with theoretical mechanisms.

Shangguan *et al.* suggested that the mechanism to maintain stable morphology of the interface at the steady-state growth rate was attributed to solute pile-up in front of the bottom of the cellular interface, and solute concentration at the bottom increased to keep constant kinetic undercooling[3)]. Higashino *et al.* reported appearance of recalescence regions in front of growing surface in phenyl salicylate (salol) by means of an in situ observation using an interferometer[4)]. Temperature and concentration gradients in the liquid become driving forces of convection in the liquid and the convection influences the morphological change of the growth interface.

Therefore, an application of a microgravity environment is a promising method to investigate the morphological stability of the growth interface. In the present paper some results of FACET (Investigation on Mechanism of Faceted Cellular Array Growth) project conducted in microgravity are reported.

2. Experimental Procedure

Crystallization of salol - *t*-butyl alcohol alloy and purified salol, which showed faceted growth interfaces, was carried out with a constant temperature gradient and with a constant cooling rate at both ends of a specimen cell. At the beginning of crystallization, the specimen was kept stationary in temperature gradient for several hours, so that a planar S/L interface was formed and the seed crystals grown up to nearly constant dimensions.

Refractive index of transparent alloy melt depends on temperature, concentration and wavelength of incident light. If change of temperature and concentration in the melt, ΔT and ΔC, are small enough, change of the refractive index Δn can be approximated by a linear function of ΔT and ΔC. Therefore, spatial distribution images of two different wavelengths, λ = 532 nm and 780 nm, are transformed into temperature and concentration distributions by solving the equation. Crystallization Observation Facility (SCOF) is a JAXA subrack facility on Kibo. It has an amplitude modulation microscope and is equipped with two-wavelength microscopic interferometer to simultaneously measure morphological change of S/L interface and distributions of temperature and concentration fields in the melt .

2. Progress of FACET Project

FACET project was completed on Oct, 2010. The growth experiments with a total of twenty parameters were performed at a constant pace. More than ten trerabytes of still images were extracted from MPEG-2 movies obtained on Kibo. The images were classified to two kinds of the interference fringe images, the bright field images, and useless images caused by block-noise and by mixture of wrong images. The images and the telemetry data of temperature were synchronized by adjusting the frame counter of the movies. Several kinds of home-made software were newly developed and were used for the data processing. The morphological change of the growth interface was obtained by outline extraction of the bright field images. The distributions of Δn for λ = 532 nm and 780 nm were calculated from the interference fringe images. Currently the growth velocity as a function of kinetic undercooling on the S/L interface and the onset of breakdown of the S/L interface were evaluated from the data.

References

1) Maby, E.W., Geis, M.W., LeCoz, Y.L., Silversmith, D.J., Mountain, R.W., and Antoniadis, D.A., *Electron. Device Lett.*, **edl-2**, 241, 1981.
2) Tokairin, M., Fujiwara, K., K. Kutsukake, Usami, N., and Nakajima, K., *Phys. Rev. B*, **80**, 174108, 2009.
3) Shangguan, D.K., and Hunt, J.D., *Metall. Trans. A*, **23A**, 1111, 1992.
4) Higashino, T., Inatomi, Y., and Kuribayashi, K., *J. Crystal Growth* **128**, 178, 1993.

”きぼう”実験でおこなう結晶成長”その場”観察実験の目的と準備状況

〇塚本勝男、山崎智也、忍健太郎、三浦均、木村勇気、吉崎泉、佐崎元

Aim and the Status of Preparation for "In Situ" Observation of Crystal Growth in KIBO

K. TSUKAMOTO, T. YAMAZAKI, K. OSHI, H. MIURA, Y. KIMURA (Tohoku Univ.),
I. YOSHIZAKI (JAXA), G. SAZAKI (Hokkaido Univ.)

In situ observation of Lysozyme crystal growth will be conducted in Kibo in 2012. The project is called as “NanoStep” in which we will measure the growth rate of crystals to understand the effect of impurities and the perfection of protein crystals in relation to the growth mechanism. Lysozyme is used as a model compound for the study. To understand the growth rate increase in space is an important aim which is related to impurity effects in the growth kinetics.

The growth rate of protein crystals is the order of 10-2nm/s and thus 4-6 magnitude of order smaller in the growth rate compared to cases of melt growth such as semiconductors, metals and ice. If the measurement is successful, that would absolutely be the smallest growth rate ever measured in space. Especially in protein crystal growth no one has succeeded to measure the rate in-situ. One of the successful measurements was our case which was done in FOTON-M3 mission by “ex-situ” method.

In order to understand the growth mechanism, we will measure the growth rate vs supersaturation using seed crystals in three solutions with different impurity concentrations. The surface of the seed crystals is chemically fixed and thus without temperature control before experiment the seeds will not be dissolved, **Fig.1**. To reveal imperfection of the crystal in relation to the growth mechanism differences, the surface of the crystals will be subjected to a slight etching, only one monolayer dissolution, leveling shallow etch pits due the incorporation of microdefects. This will be done after every growth experiment. This is also the first experiment in space.

We will employ Michelson interferometer for the measurement of growth rate from the surface of the crystal, the reflectivity of which is less than 1% and thus we need special geometrical arrangement in the growth cell. The temperature will be changed from 5-40 degree C.

The miniaturized growth cell and optics are shown in **Fig.2**. These are installed in the ESCOF system in JEM in such a way that we can measure the concentration gradient around the crystal along a vertical direction. One of the test Michelson images from the surface is shown in **Fig.3**.

In the talk, we will discuss about both scientific and technical/engineering problems.

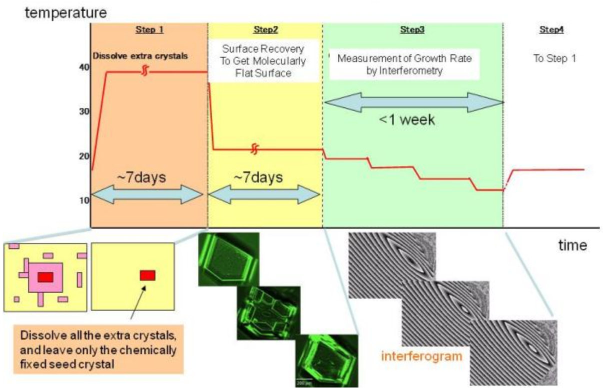

Fig. 1 Experimental schedules for NanoStep project. Three weeks are needed for one experiment.

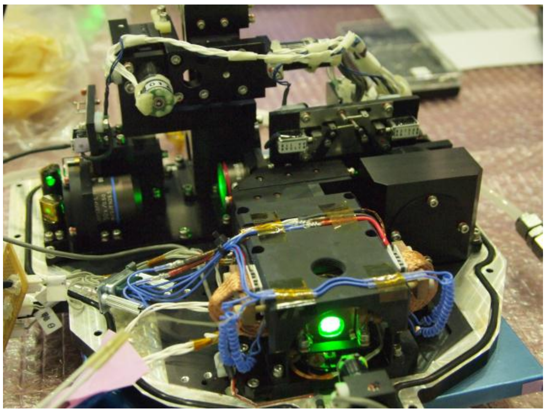

Fig. 2 Experimental setup. The cell in front and the optics in rear. Green laser is used for higher reflection from the crystal surface.

Fig. 3 Michelson interferogram from a Lysozyme. Note a straight grain boundary separating the surface into two parts.

S-520 観測ロケットを用いた宇宙ダストの再現実験にむけて: 干渉計を用いた核生成のその場観察

木村勇気，○三浦均，塚本勝男(東北大学)，稲富裕光（JAXA)

Toward a Reproduction Experiment of Cosmic Dust using S-520 Observation Rocket: In-Situ Observation of Nucleation by Interferometer

Yuki KIMURA, Hitoshi MIURA, Katsuo TSUKAMOTO (Tohoku Univ.), Yuko INATOMI (JAXA)

1. Introduction

To understand the formation process of cosmic dust particles (dust) with nm to sub-μm in size, dust analogues have been produced in the laboratory. The gas evaporation method has a similarity in the dust formation process in space, where dust forms by a condensation from gas phase via homogeneous nucleation in some case. However, nucleation process has been unknown not only in universe but also in the laboratory. Recently, we succeeded in directly observing the temperature and concentration during homogeneous nucleation in the vapor phase by interferometer under the gravity.[1,2] To understand the homogeneous nucleation quantitatively, we applied nucleation theories to the experimental results and obtained the following results: the surface free energy, the size of critical nuclei, temperature profile of nuclei related to the latent heat, determination of polymorph, fusion growth and order of sticking probability. Here, we will show the future experiment in μG using an observation rocket. μG experiment has an advantage to determine above mentioned values more certainly.

2. Experimental setups

Smoke particles of WO_3, SiO, Mn, Fe, Au or NaCl were produced in a specially designed smoke chamber containing a Mach–Zehnder-type interferometer with two wavelengths lasers, which can obtain two unknown parameters simultaneously, i.e., concentration of evaporated vapor and ambient temperature.

When an evaporant is initiated in an inert gas, the evaporated vapor subsequently cools and condenses in the gas atmosphere, i.e., nanoparticles are obtained via homogeneous nucleation from the vapor phase. In this manner, nucleation will occur far from the equilibrium state, but it is not obvious how far condensation takes place. The smoke particles were directly collected on an amorphous thin film of carbon mounted on a standard transmission electron microscope (TEM) grids. The size and number density of the condensed particles are determined by a TEM observation.

3. Results under the gravity experiments

In case of Mn and WO_3, condensation occurred at 660 K and 600 K below the equilibrium temperatures, and the degree of supersaturation was as high as 10^5 and 10^9, respectively.

The condensation temperature, number density, and size of particles for Mn experiment were consistent with the values calculated by the semi-phenomenological nucleation theory. On the other hand, however, the results have a gap with the values calculated by the nucleation theories in case of WO_3 and NaCl. One of the reasons may be due to secondary growth. Since there is strong thermal convection generated by the hot evaporation source in the chamber, condensed particles follow the convection and possibly grow in the way as gas cools. As the result, size and number density could be different from the theory. In the same reason, sticking probability, which is estimated from the growth rate, can be obtained more certainly.

4. Microgravity experiment

In this year, we firstly performed the gas evaporation experiments in μg using the aircraft, G-II, of DAS. Here, we will present the brief results and show the difference from gravity experiment toward a reproduction experiment of cosmic dust using an S-520 observation rocket, which generates μg more than 5 min. Since μg environment strongly suppresses the thermal convection, evaporated vapor diffused simply to the direction of centric distance and condensed at the wider area compared with gravity condition due to no convection as shown in **Fig. 1**. Then, it can be concluded that condensation in μg is more difficult than that in gravity, i.e., condensation occurred far from the evaporation source. Since condensation and growth in μg occur at the same place, secondary growth is negligible and the results are able to compare with the formation of cosmic dust particles.

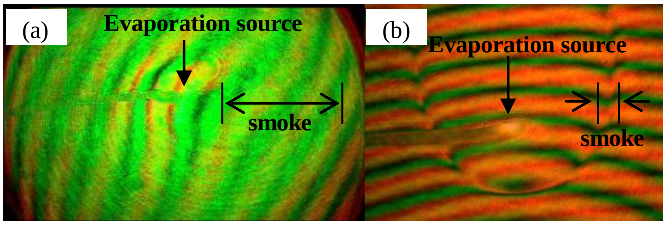

Fig. 1 Double wavelength interferogram of WO_3 smoke produced by an evaporation of W in a mixture gas of Ar and O_2 in (a) μg and (b) gravity. Thick of W wire is the same in both images, ϕ0.3 mm.

References

1) Y. Kimura, and K. Tsukamoto, *J. Jpn. Soc. Microgravity Appl.*, (2011) in press.

2) Y. Kimura, H. Miura, K. Tsukamoto, C. Li, and T. Maki, *Journal of Crystal Growth*, **316** (2011) 196.

微小重力下での $Si_{0.5}Ge_{0.5}$ 結晶成長実験計画

○木下恭一、荒井康智、稲富裕光(JAXA)、宮田浩旭、田中涼太(エイ・イー・エス)、
塚田隆夫(東北大学)、高柳昌弘、依田眞一(JAXA)

Plan for $Si_{0.5}Ge_{0.5}$ Growth Experiments in Microgravity

K. KINOSHITA, Y. ARAI, Y. INATOMI(JAXA), H. MIYATA, R. TANAKA(AES),
T. TSUKADA(Tohoku Univ.), M. TAKAYANAGI, S. YODA(JAXA)

1. Introduction

We have invented a new crystal growth method named as traveling liquidus-zone (TLZ) method, which enabled us to grow compositionally uniform alloy crystals[1-3]. Since the TLZ method requires diffusion limited mass transport, TLZ grown crystals are limited to small diameter or thin plate in order to suppress convection in a melt on the ground. For device applications, large diameter crystals are required. We therefore applied crystal growth experiments on board the ISS "Kibo".

2. Aims of Space Experiments

$Si_{0.5}Ge_{0.5}$ crystal growth by the TLZ method will be performed in microgravity with suppressing convection in a melt. Aims of space experiments are evaluation of two-dimensional TLZ growth model[4] and attainment of knowledge for large diameter homogeneous ally crystals by the TLZ method. We think that radial temperature gradient causes compositional inhomogeneity and control of radial temperature gradient is important for large diameter crystal growth. $Si_{0.5}Ge_{0.5}$ crystals are promising as substrates for high speed and low energy consumption electronic devices and large homogeneous crystals are expected.

3. Outline of space Experiments

Principle of the TLZ method is shown in **Fig. 1**. A Ge-rich melt zone is formed between a Si seed and a Si feed. Since temperature gradient determines growth rate in the TLZ method, maintaining constant temperature gradient is important. Three experiments at 7℃/cm and one experiment at 14℃/cm are planned using a gradient heating furnace (GHF). For growing $Si_{0.5}Ge_{0.5}$ crystals, growth interface temperature will be kept at 1100℃. Growth rate is about 0.1 mm/h for a temperature gradient of 7℃/cm. For keeping constant growth interface temperature, heaters are translated in accordance with growth interface shift.

Heater length of the GHF is rather short comparing with conventional laboratory furnaces and maintaining constant temperature gradient is more difficult. In space experiments, heater temperatures are pre-set as a function of time and very precise temperature control is required. Therefore, the sample obtained by the first experiment will be returned to the earth and compositional profiles are analyzed before second experiment. Preset temperature data will be adjusted based on the first experiment and improved compositional uniformity will be attained in the later experiments.

4. Summary

Samples and the GHF have already been launched by HTV II (Kounotori) in January 2011. When checkout of the GHF is completed, crystal growth experiments will be begun. We hope that TLZ growth experiments are successful and we obtain fruitful data for growing large homogeneous alloy crystals by the TLZ method.

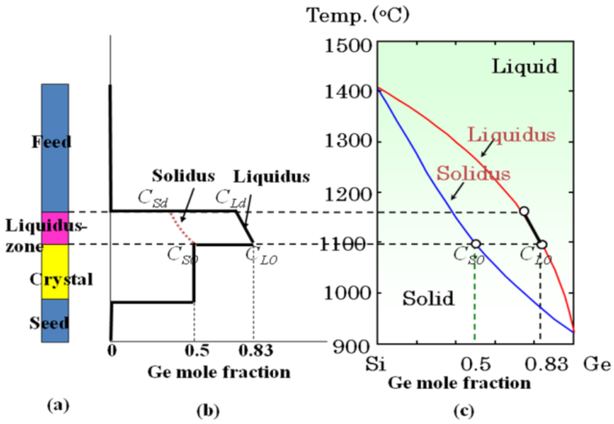

Fig. 1 Principle of the TLZ method, (a) sample configuration, (b) Ge concentration profile (c) phase diagram of the Si-Ge system.

References

1) K. Kinoshita, H. Kato, M. Iwai, T. Tsuru, Y. Muramatsu, and S. Yoda, J. Crystal Growth, **225** (2001) 59..

2) H. Nakamura, Y. Hanaue, H. Kato, K. Kinoshita and S. Yoda, J. Crystal Growth, **258** (2003) 49.

3) K. Kinoshita and S. Yoda, J. Crystal Growth, **318** (2011) 1026.

4) S. Adachi, K. Kinoshita, M. Takayanagi and H. Miyata, J. Crystal Growth, .**334** (2011) 67.

長期宇宙滞在を目的とした空気再生系における市販ルテニウム触媒を用いたサバチエ反応

○伊藤由紀仁，鈴木進補（早稲田大学），島明日香，桜井誠人，大西充（JAXA）

Sabatier Reaction using Commercial Ru Catalyst in an Air Revitalization Device Developed for Long Term Space Stay

Yukihito ITO, Shinsuke SUZUKI (WASEDA Univ.), Asuka SHIMA, Masato SAKURAI, Mitsuru ONISHI (JAXA)

1. Introduction

CO_2 reduction is hoped as advanced closer air revitalization system in International Space Station (ISS) and any other manned space missions. Recently, a CO_2 reduction device based on following Sabatier reaction is being developed.

This reaction reduces CO_2 by H_2 over a Ru-loaded metal oxide catalyst and generates CH_4 and H_2O gases (eq 1). According to the previous research[1] a heater is necessary to keep the exothermic reaction because the most efficient temperature for this reaction is known to be ranging from 350 to 400 ^{o}C. Development of CO_2 reduction devices for space missions requires scale-up to the practical use, high conversion rate, additional downsizing and energy saving.

$$CO_2 + 4H_2 \xrightarrow[\text{heat}]{\text{Ru catalyst}} CH_4 + 2H_2O \qquad (1)$$

JAXA has already clarified that the relationships between CO_2 flow rate and conversion rate, catalyst temperature with a bench-scale model.[2]. In this study, we investigated the relationship between the conversion rate of CO_2 reduction device and the catalyst amount using a scaled-up reactor.

2. Experimental

Commercial Ru catalyst (0.5wt% Ru/Al_2O_3 N.E.Chemcat) of 16g, 32g, 48g, and 64g was set in a reactor of stainless steel cylindrical with an inner diameter of 25mm (**Fig.1**). Thermocouples were positioned as shown in Fig.1 to obtain the temperature distribution of the catalyst. The reactor was heated from the outside by a heater. The reaction gas mixture of CO_2 and H_2 was flowed through the reactor at a given flow rate of 350:1400 or 350: 910 ml/min. The reaction effluent from the gas outlet of the reactor was analyzed with a gas chromatograph during the experiment under each experimental condition of the flow rate and catalyst amount. The conversion of CO_2 was calculated from the concentrations of CO_2 and CH_4.

3. Results and Discussion

The conversion rate of CO_2 increased with increasing amount of catalyst and H_2 flow rate (**Fig.2**). The highest conversion rate of 90% and 62% were achieved when the catalyst amount was 64g at both flow rates.

The temperature increased from Pos.1 to 2 and decreased from Pos.2. The result shows most of the reaction finished in the vicinity of the gas inlet.

4. Summary

The CO_2 reduction device in this study showed a conversion rate as high as the small reactor (1/10 person) at the flow rate of 350:1400 ml/h. As only the catalyst near the gas inlet is considered to be necessary for CO_2 reduction, there is room for downsizing of the reactor.

References

1) P. J. Lunde and F. L. Kester, Ind. Eng. Chem., Process Des. Develop., **13**-1(1974)27.
2) K. Usuku, S. Toda, M. Sakurai A. Shima, M. Onishi, and S. Yoshihara. 54th Proc. Space Sci. Technol. Conf. Shizuoka, JPN, Nov. 2010, 4299.

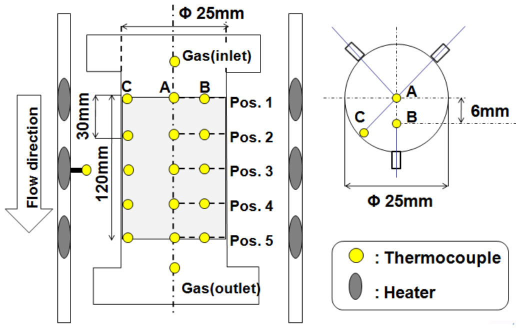

Fig.1 Schematic illustration of Ru catalyst reactor.

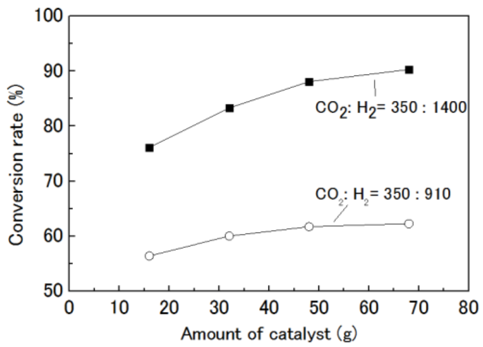

Fig.2 Relationship between the conversion rate of CO_2 and the amount of catalyst in the reduction device

28A06

次世代型水再生装置の開発

○小口美津夫、桜井誠人、大西充、島明日香 (JAXA)

Development of a Next Generation Type Water Recovery System

Mitsuo OGUCHI, Masato SAKURAI, Mitsuru OHNISHI, Asuka SHIMA (JAXA)

1. Introduction

JAXA is working in the development of a compact, low power water recycling device that can supply delicious drinking water which can be consumed safely and with peace of mind in order to help astronauts lead a healthy and comfortable life in space. This device uses electrolysis to decompose ammonia and organic matter, purifies the water using a reverse osmosis membrane, adds minerals to the water, and then sterilizes the water, thereby maintaining water quality. An online system for measuring TOC and harmful substances is also used to manage the water quality.

2. The current status and issues with NASA water recycling system

NASA system is composed with vapor compression distillation, in which urine is evaporated and the water vapor condensed to form distilled water, and membrane processing to recycle domestic wastewater.

With the NASA method, there is the problem of ammonia components remaining in the water. There is also a high level of electric power consumption, at approximately 1 KW. Furthermore, there are many parts that require periodic replacement, such as membrane cartridges and ion exchange resin, so the system will require 26 hours of maintenance per year.

3. Determination of Equipment Specifications, and Design Study

The goal of this development is to achieve a water purifying system based on reverse osmosis (RO) membranes. Preprocessing that decomposes ammonia and organic matter contained in urine. Post-processing that adds minerals and sterilizes the water.

A study of the components of urine shows that urine contains ammonium ions (NH_4^+) at a ratio of approximately 1,000 ppm [1]. Ammonia (ammonium ions) can be removed by a reverse osmosis membrane, but in an alkaline aqueous solution, the ammonia becomes ammonia gas and dissolves, and this gas can easily pass through a reverse osmosis membrane. Therefore, in this research and development project, we examined the direct dissociation of the ammonia.

4. Ammonia dissociation test

Ammonium chloride and sodium chloride were used to prepare an evaluation solution (raw water) containing 1,000 ppm ammonium ions (NH_4^+) and 7,000 ppm chlorine ions (Cl^-). An electrolysis cell was prepared using an iridium electrode for the positive electrode and a platinum electrode for the negative electrode.

Figure 1 shows the results of the electrolysis test. In this test, two pairs of electrodes were used in combination to prepare the electrolysis cell, so the electric power supply to the cell was 5.4 V DC, 10A x 2.

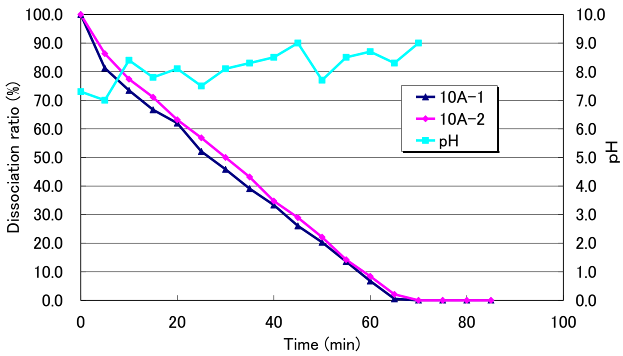

Fig. 1 Ammonia dissociation ratio

In this test, the pH of the raw water was controlled at a suitable level, so the hypochlorous acid ions that disassociate the ammonium ions remained present continuously.

5. Conclusion

In this study, we have examined the removal of ammonia, a fundamental element of the device being developed. It was found that with electrolysis, an ammonia component of 1,000 ppm (equivalent to that of urine) could be reduced to zero in 70 minutes. We anticipate that dissociation efficiency can be further increased and electric power consumption decreased through measures such as decreasing the distance between electrodes, increasing the electrode surface area, and reducing the resistivity of the wiring and electrical contacts. It was also verified that the electrolysis cell used to remove ammonia could also be used for TOC removal, making it possible to simplify the system.

References

1) Test to Acquire Fundamental Data Related to Actual Urine, NASDA Results Report GAE-96002, 1996.

新たな宇宙服関節部形状の提案とその屈曲特性

○池間賢吾，グバレビッチアンナ，小田原修 (東京工業大学)

Bending Property of Newly Designed Joint for Spacesuits

Kengo IKEMA, Anna V. GUBAREVICH, Osamu ODAWARA (Tokyo Institute of Technology)

1. Introduction

Future manned long-term missions on lunar and Martian surfaces will need more advanced extravehicular operations to enable in-space construction of complex facilities and habitant modules. As well as life support functions to survive in harsh space environment, spacesuits should enhance human potential physical abilities for advanced EVA operations. Among various capabilities that spacesuits need to possess, suit joints' mobility with low resistance and wide range of motion is particularly important for long and complex operations wearing suits. However, joint flexibility of current suits is not guaranteed sufficiently because high pressure difference across the garment induces strong tensile force and makes soft material stiff [1].

This study has developed new design of single-axis joint made of soft material to provide high flexibility. Joint prototypes were fabricated and bending properties were investigated.

2. New Design of Spacesuit Joint

The proposed joint is based on one particular oblate spheroidal shape that theoretically carries interior pressure purely by meridional stress, i.e. circumferential stress is zero everywhere [2]. Introducing excess skin material into the oblate spheroid along circumferential direction by inserting the extra number of gores generates local slack regions, which enables extraction and contraction resulting in flexion motion with low resistance torque. Furthermore, the geometry of the joint is axisymmetric so that the envelope maintains constant inner volume throughout the full joint range of motion, which eliminates pressure-volume work.

To incorporate the oblate spheroidal shape to single-axis joint, two cylindrical parts corresponding to arms are merged on lateral surface of oblate spheroid.

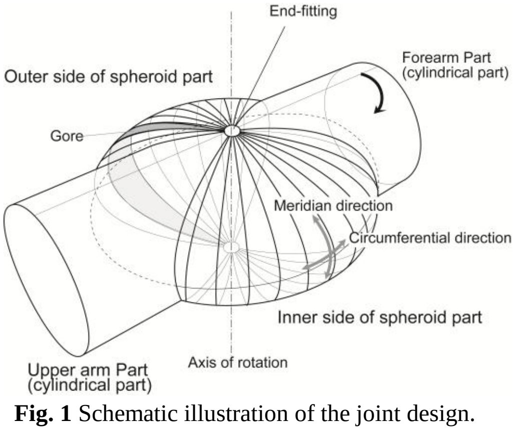

Fig. 1 Schematic illustration of the joint design.

3. Experimental

To investigate flexion characteristics, joint prototypes were fabricated from silicone-rubber coated Vectran woven fabric and subjected to flexion tests using a custom-made robotic arm. Both ends of joint prototype were fixed and sealed on robotic arm and pressurized inside to initial inner pressure value. Then, robotic arm was quasi-statically flexed and extended.

From the shape observation as shown in **Fig. 2(a)**, the presence of excess skin which enables extraction and contraction are confirmed, which effectively gives rotational flexibility. Results of torque measurement (see **Fig. 2(b)**) shows that torque increased mildly when flexion angle was increased from 20° to 80°, and it started to rise rapidly at higher angles. Rapid torque increase at higher angles is explained by undesired deformation of both cylindrical parts.

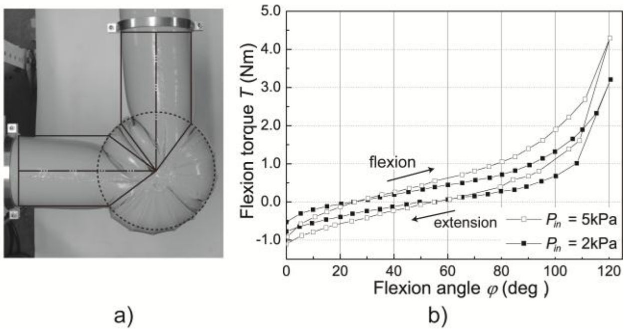

Fig. 2 Typical experimental results: a) the photograph of arm joint flexion at 90° (top view), b) the relationship between flexion angle and torque. P_{in} is initial inner pressure.

4. Conclusion

It was concluded that the presence of excess skin could effectively provide flexibility at low angles, and high torque at higher angles should be addressed in the future design improvement.

References

1) D. Newman, M. Barratt, Life Support and Performance Issues for Extravehicular Activity, in: Churchill SE (Ed.), Fundamentals of Space Life Sciences (1997).

2) G.I. Taylor, On the shape of parachutes, in: G.K. Batchelor (Ed.), The Scientific Papers of Sir G.I. Taylor, Vol. III (1963).

スペースコロニー内の人工重力下における大気循環の解析

〇宮嶋宏行 (東京女学館大学)

Air Circulation Analysis under Artificial Gravity in a Space Colony

Hiroyuki Miyajima (Tokyo Jogakkan College)

1. Introduction

A typical space colony is cylinder in shape. It was first proposed by G. O'Neill in 1974 and named "Island Three". The diameter is 6km, the length is 30km, and ten million people are able to live in the colony. The cylinder is rotated 0.55rpm to create an artificial gravity of 1g. The inside wall of the cylinder is divided into six sections in an axial direction, which consists of three sections of habitable land and three non-habitable window sections alternately. Each window outside has a movable mirror installed to reflect sun light. It can artificially create days, nights, and seasons[1).

The previous space colony research falls into several categories. Although there has been much research in the dynamics and structure analysis of the space colony, little research has been done concerning internal environmental analysis. There were few research projects, which took into account meteorology in a space colony[2) and rotating dishpan experiment of the air circulation[3). The results predict that the temperature difference between the land sections and window sections, along with the Coriolis force cause the air circulation by window-wind from the window sections to the land sections in a space colony.

The purpose of this research is the air circulation analysis caused by the window-wind in a space colony which takes into account humans, crops, and waste process factories.

2. Modeling and Analysis

The internal space on the shell of the space colony is divided into ground and atmospheric layers. Each layer is divided into 100 x 60 cubic cells having physical quantities such as concentration of N_2, O_2, and CO_2. Each cell has almost equal sides of 300 m in length. The changes of concentrations are modeled by using Cellular Automaton (CA). The equations (1)-(3) represent the CO_2 diffusion and advection model, and the photosynthesis models in light and dark periods, respectively.

$$\frac{\partial(ppCO_2)}{\partial t}=D\left(\frac{\partial(ppCO_2)}{\partial x}+\frac{\partial(ppCO_2)}{\partial y}\right)+v_x\frac{\partial(ppCO_2)}{\partial x}+v_y\frac{\partial(ppCO_2)}{\partial y} \quad (1)$$

$$mCO2(t+1)=mCO2(t)+(-CO2\_PHO\cdot biomass+CO2\_POP\cdot population) \quad (2)$$

$$mCO2(t+1)=mCO2(t)+(CO2\_DAR\cdot biomass+CO2\_POP\cdot population) \quad (3)$$

3. Results and Discussion

The space colony could support seven million people and 30 species of crops such as rice, soybeans. These crops could be cultivated to support the population. The mirrors are opened from 5:00 to 7:00, which is dawn, and closed from 17:00 to 19:00, which is dusk. CO_2 emission from the waste process factory is released from 7:00 to 17:00 at point 1.

Figure 1 shows the distribution of CO_2 concentration at 5:10 on day 2. The maldistribution of CO_2 concentration begins to be stirred up by window-wind in each window-land pair when mirrors begin to open. **Figure 2** shows changes in CO_2 concentration in 48 hours at points 1, 51, and 91. The abrupt decrease of CO_2 concentration at 5:10 on day 2 at three places was caused by the window-wind. The concentration decreased to the first CO_2 concentration at 0:00 of the previous day.

I have formulated and analyzed the air circulation in a space colony using a CA. I am engaged in the preparation of experiments of window-wind under artificial gravity.

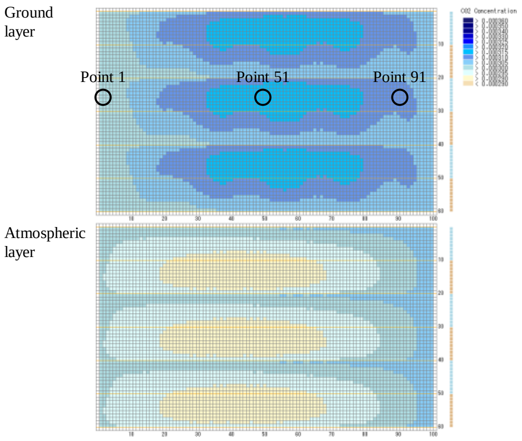

Fig. 1 Distribution of CO_2 concentration at 5:10 on day 2

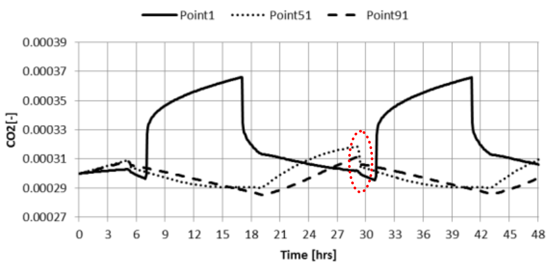

Fig. 2 Changes in CO_2 concentration in 48 hours

References

1) G. K. O'Neill, The High Frontier: Human Colonies in Space 3rd Edition, Collectors Guide Pub, 2000.

2) T. Matsuda, Meteorology in a Space Colony, Journal of the Physical Society of Japan, **52**, 6, (1983)1904-1907.

3) T. Yoshimura, On the Meteorology in a Space colony, The Astronomic Herald, **85**, 11(1992)509-514.

1G 環境下における温度勾配炉を用いた $In_xGa_{1-x}Sb$ 混晶半導体結晶成長

○早川泰弘, M. ARIVANANDHAN, G. RAJESH, 田中 昭 (静岡大学), 小澤哲夫 (静岡理工科大学),
岡野泰則 (大阪大学), 阪田薫穂, 稲富裕光（宇宙航空研究開発機構）

Growth of $In_xGa_{1-x}Sb$ alloy crystal using Gradient Heating Furnace under 1G condition

○Yasuhiro HAYAKAWA, Mukannan ARIVANANDHAN, Govindasamy RAJESH, AkiraTANAKA
(Shizuoka Univ.), Tetsuo OZAWA (Shizuoka Institute of Science and Technol.),
Yasunori OKANO (Osaka Univ.), Kaori SAKATA, Yuko INATOMI (JAXA)

1. Introduction

$In_xGa_{1-x}Sb$ is a potential ternary alloy semiconductor with narrow band gap and it is mainly useful for thermo photovoltaic (TPV) application[1]. However, solute and heat transport due to complex convection induced by gravity makes the crystal growth of homogeneous $In_xGa_{1-x}Sb$ as a difficult task[2]. Since the solute transport is affected by convection, the dissolution and growth processes are strongly influenced by gravity.

In the present work, growth of $In_xGa_{1-x}Sb$ crystal using Gradient Heating Furnace (GHF) is demonstrated as a preliminary experiment for microgravity experiment at International Space Station (ISS).

2. Experimental method

To prepare seed and feed crystals for GaSb(seed)/InSb/GaSb(feed) sandwich sample, GaSb single crystals with different orientations viz., (100), (110), (111) were grown by CZ method. As a preliminary growth experiment, InGaSb crystal was grown under 1G condition using the GHF furnace. The orientation of the GaSb seed was fixed as (111)A for the present experiment. The sandwich structured sample filled ampoule was sealed at high vacuum. The ampoule was placed in GHF and heated upto 690°C under the temperature gradient of 0.57°C/mm. The Te impurity concentration was modulated by applying heat pulses thereby striations were formed in the grown ingot. Growth rate was calculated by measuring the distance between the striations which are revealed by etching the grown crystal surfaces using CH_3COOH : HF : $KMnO_4$ (1:3:1).

3. Results and discussion

Figure 1 shows the composition profile of the growth crystal and the cross section view of the crystal. The In composition was gradually decreased along the grown length and fluctuated after 31.6 mm due to rapid solidification of residual solution during post-growth cooling. When the growth proceeds, the growth interface moves towards high temperature and thus the In composition decreases. The growth rate was measured from the observed growth striations and the maximum growth rate of 0.16mm/h was observed at the grown length of 4.7 mm.

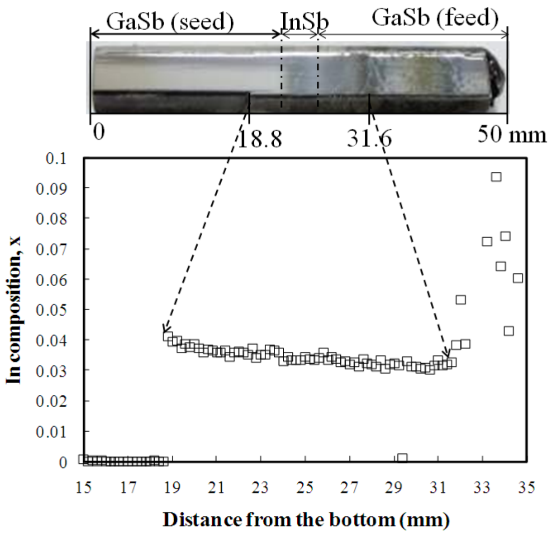

Fig. 1 Indium compositional profile of the grown sample.

4. Conclusion

The growth condition and temperature profile were optimized in the GHF furnace for the growth of $In_xGa_{1-x}Sb$. The same experimental conditions will be employed for the future experiments in 1G and microgravity conditions at ISS.

References

1) N. Murakami, K. Arafune, T. Koyama, M. Kumagawa, Y. Hayakawa: J. Cryst. Growth 275 (2005) 433.
2) K.M. Kim, J. Cryst. Growth Vol. 44 (1978), p. 403.

数値解析を参考にした微小重力環境での高品質タンパク質結晶生成条件の最適化

○田仲広明(コンフォーカルサイエンス)、伊中浩治、古林直樹(丸和栄養食品)、山中麻里、高橋幸子(コンフォーカルサイエンス)、佐野智、太田和敬、小林智之、吉村善範(JAXA)

Optimization of Crystallization Condition to Grow Higher Quality Protein Crystals in Microgravity Based on Numerical Analysis

○Hiroaki TANAKA (Confocal Science Inc.), Koji INAKA, Naoki FURUBAYASHI (Maruwa Foods and Biosciences Inc.), Mari YAMANAKA, Sachiko TAKAHASHI (Confocal Science Inc.), Satoshi SANO, Kazunori OHTA, Tomoyuki KOBAYASHI, Yoshinori YOSHIMURA (Japan Aerospace Exploration Agency)

1. Introduction

It is said that there are positive effects of microgravity on higher quality protein crystal growth. The formation of a protein depletion zone (PDZ) and an impurity depletion zone (IDZ) due to the suppression of a convection flow were thought to be the major reasons[1)]. In microgravity, the incorporation of the molecules into the crystal highly depends on the diffusive transport, so that the incorporated molecules may be allocated in order and the impurity uptake may be suppressed, resulting in highly ordered crystals. We studied those effects numerically using a simplified model, and we applied the results of the numerical analysis to the estimation of microgravity effects on protein crystal growth before performing microgravity experiments.

2. Numerical Analysis

PDZ effect can be expressed as the driving force ratio (DFR) for microgravity (0G) vs. ground-based (1G),

$$DFR = \frac{DFR_{0G}}{DFR_{1G}} = \frac{C(R) - Ce}{C(\infty) - Ce} = \frac{1}{1 + \dfrac{R \cdot \beta}{D}} \quad (1)$$

where C(∞), C(R) and Ce (mg/ml) are the concentrations of the protein far away from the crystal, the protein on the surface of the crystal and of the protein solubility, respectively; β is a kinetic coefficient for the protein molecule; D is a diffusion coefficient of the protein molecule; and R is the radius of the crystal. The growing crystal was presumed to be a sphere.

IDZ effect can be expressed as the impurity uptake ratio (IR), which is the ratio of the impurity uptake during the crystal growth in microgravity (IUR_{0G}) and on the ground (IUR_{1G}),

$$IR = \frac{IUR_{0G}}{IUR_{1G}} = \frac{\dfrac{\beta i \cdot Ci(R)}{\beta \cdot (C(R) - Ce)}}{\dfrac{\beta i \cdot Ci(\infty)}{\beta \cdot (C(\infty) - Ce)}} = \frac{1 + \dfrac{R \cdot \beta}{D}}{1 + A \cdot \dfrac{R \cdot \beta}{D}} \quad (2)$$

$$A = \frac{\beta i \cdot D}{\beta \cdot Di} \quad (3)$$

where β_i was a kinetic coefficient for impurity trapped in the crystal; D_i was a diffusion coefficient of the impurity molecules; and $C_i(R)$ and $C_i(\infty)$ were the concentrations of the impurity on the surface of the crystal and far away from the crystal, respectively. D and β values could be obtained by simple experiments.

As shown in these equations, a lower D/β and a larger R could work to enhance the filtering effects of protein and impurity by forming a PDZ and IDZ. Therefore, we applied D/β values to expect the microgravity effects on growing good crystals before performing microgravity experiments.

3. Crystallization in Microgravity

Totally more than 150 protein samples were launched in JAXA PCG#1, #2 and #3 flight experiments. The number of protein samples whose D/β value were estimated was 45, and the number that were successfully grown to larger single crystals was 25. Their crystal radius was usually over 0.1 mm. Crystal quality was judged by the maximum X-ray resolution and/or the mosaicity of the crystals in this study. The rate of the effective samples was higher if the D/β value was lower, as expected. When the D/β value was less than 3 mm, more than 75% of the samples were positively affected by the microgravity environment to grow higher quality crystals.

4. Conclusions

We developed simple methods to estimate D and β. Using these values, we can utilize the microgravity environment effectively to obtain high-quality protein crystals. More positively, we prepared a highly purified protein sample to make β higher and a high-viscous crystallization solution to make D lower. So far, most of the crystals were for X-ray diffraction crystallography in our experiments. Therefore, the crystal radius did not usually affect to increase the Rβ/D values. So the IDZ rather than the PDZ could be expected. We applied this strategy to the crystallization experiments of various proteins such as hematopoietic prostaglandin D synthase[2)], lipocalin-type prostaglandin D synthase[3)], lysozyme, etc.,and successfully obtained higher-quality crystals in microgravity.

References

1) H. Tanaka, K. Inaka, S. Sugiyama, S. Takahashi, S. Sano, M. Sato, and S. Yoshitomi: Ann. N.Y. Acad. Sci., **1027** (2004) 10.

2) H. Tanaka, T. Tsurumura, K. Aritake, N. Furubayashi, S. Takahashi, M. Yamanaka, E. Hirota, S. Sano, M. Sato, T. Kobayashi, T. Tanaka, K. Inaka, and Y. Urade: J. Synchrotron Rad., **18** (2011) 88.

3) K. Inaka, S.Takahashi, K. Aritake, T.Tsurumura, N. Furubayashi, B. Yan, E. Hirota, S. Sano, M. Sato, T. Kobayashi, Y. Yoshimura, H. Tanaka, and Y. Urade: Cryst. Growth Des. **11** (2011) 2107.

28B07

微小重力下一方向凝固による n-型 Si-Ge 熱電材料の合成

○奥谷　猛，壁谷侑篤，濱田　剛（横国大），永井秀明（産総研）

Thermoelectric n-type Si-Ge synthesized by unidirectional solidification in microgravity

Takeshi OKUTANI, Yuuto KABEYA , Tsuyoshi HAMADA (Yokohama National University), Hideaki NAGAI (AIST)

1. Introduction

Si-Ge alloy semiconductors are the most well-known materials for thermoelectric power generators at high temperature (900 to 1200K) because these materials exhibit low thermal conductivity at high temperature.[1,2] High-energy conversion efficiency (i.e., high dimensionless figure of merit ($ZT=S^2\sigma T/\kappa=PT/\kappa$; Z, figure of merit [K^{-1}]; S, Seebeck coefficient [VK^{-1}]; σ, electrical conductivity [Sm^{-1}]; κ, thermal conductivity [$Wm^{-1}K^{-1}$]; P, power factor [$wm^{-1}K^{-2}$])) should be achieved for further application such as environmentally-friendly power generator systems utilizing waste heat from energy-related facilities.

Uniform Si-Ge is produced by zone melting method or powder metallurgical method because of semiconductors. Si-Ge is a complete solid solution system and the temperature difference between liquidus and solidus lines at one composition exists, so that unidirectional solidification can make dendrite structure aligned with solidification direction which Si content decrease continuously from the dendrite center to the dendrite edge of the Ge-rich secondary arms of the dendrite. The thermoelectric properties of the Si-Ge with aligned dendrites is thought to be superior to uniform Si-Ge because Ge-rich Si-Ge has low thermal conductivity and high electrical conductivity. In microgravity, the dendrite structure is easy to align along cooling direction by unidirectional solidification, because of no convection in melt and no hydrostatic pressure. The Si-Ge with the oriented dendrite structure is thought to have an anisotropy of thermoelectric properties. In this report, unidirectional solidification of Si-Ge in microgravity was conducted to synthesize Si-Ge with oriented dendrite structure, and the thermoelectric properties of solidified products were measured.

2. Experimantal

Starting sample of Si-Ge was prepared by arc-melting of Si and Ge (Si:Ge=8:2 and 7:3 (atomic ratio)). P is added to the Si and Ge grains to adjust 1 at% for Si-Ge of ingot after arc-melting. The sample was heated by IR furnace to melt completely at 1643K for 20s. Unidirectional solidification process was conducted by contact with the copper chill block. The microgravity experiments were performed using 2m-drop tower to obtain microgravity of ±0.05g for 0.46s. The furnace was switched off just after free fall of the equipment, and the melt sample was contacted with the Cu chill block after 0.05s of the free fall. The obtained samples were analyzed by X-ray diffraction (XRD), optical microscopy (OM), scanning electron microscopy (SEM), energy-dispersive X-ray diffraction (EDX), and their electrical conductivity, Seebeck coefficient and thermal conductivity were measured as thermoelectric properties.

3. Results and discussion

The SEM photographs of section surface parallel to the cooling direction of $Si_{0.8}Ge_{0.2}$ with 1 at% P solidified unidirectionally in 1g and μg indicated dendrites were aligned along cooling direction. The width of column of the 1g sample was smaller than that of the μg sample. From the results of element distribution analysis by EDX, the inside of dendrite was Si-rich and the edge of columns was Ge-rich, and the distributions of Si and Ge in μg sample were separated clearer than that in 1g sample because of no convection.

The size of sample solidified in μg was 10mm in diameter and a thickness of 0.5mm because of μg periods of 0.45s. Therefore, the thermal conductivity (κ) of the sample along cooling direction, that is, the direction of primary arm of dendrite could be measured, and the electrical conductivity (σ) and Seebeck coefficient (S) could be measured on the sample perpendicular to cooling direction, that is, the direction perpendicular to the dendrites and columnar growth directions. For the sample solidified in 1g, the σ and the Seebeck coefficient could be measured on the both directions because thick sample, which is enough size to measure σ and S, can be produced in 1g, but the thermal conductivity could be measured on the sample direction along cooling direction only. The σ along the cooling direction of the Si-Ge with 1 at% P solidified in 1g was 1.45 to 1.55 times as high as that perpendicular to the cooling direction. The S of Si-Ge along the both directions solidified in 1g was the same.

On the base of the anisotropy between σ of the $Si_{0.7}Ge_{0.3}$-1at%P parallel and perpendicular to the solidification direction solidified in 1g, σ of the $Si_{0.7}Ge_{0.3}$-1at%P parallel to the solidification direction solidified in microgravity was estimated. *ZT* of the direction along the solidification direction of the $Si_{0.7}Ge_{0.3}$-1at%P sample solidified in microgravity was 1.19 at 1000K. The *ZT* of 0.775 has reported as the highest *ZT* for n-type Si-Ge thermoelectric material[3].

References

1) B.Abeles, D.S.Beers, G.D.Cody and J.P.Dismukes, *Phys.Rev.* 125, 44 (1962).
2) B.Abeles and R.W.Cohen, *J.Appl.Phys.* 35 , 247 (1964) .
3) C.B. Vining, in: D.M. Rowe (ed.), Silicon Germanium ---CRC handbook of thermoelectrics, CRC Press, Boca Raton, 1994, p.329-337.

異なる配向性を有する ZrNiSn ハーフホイスラー合金の合成

○永井秀明(産業技術総合研究所)，室井良太、奥谷　猛（横浜国立大学大学院環境情報研究院）

Synthesis of ZrNiSn Half-Heusler Compounds with Different Crystalline Alignment

Hideaki NAGAI(National Institute of Advanced Industrial Science and Technology [AIST]), Ryota MUROI,
Takeshi OKUTANI (Graduate School of Environment and Information Sciences, Yokohama National Univ. [YUN])

1. Introduction

The ZrNiSn half-Heusler compouds have been of interest due to their potential as thermoelectric materials. The half-Heusler compounds usually have been prepared by arc-melting and sintering the crushed arc-melting sample. Therefore the obtained sample had no crystalline alignment. We have been succeeded to directly prepared the crystalline-aligned Laves phase compounds, such as $TbFe_2$ and $SmFe_2$ etc.[1),2)], by unidirectional solidification in short-duration μg. In this study, we study the synthesis of crystalline-aligned ZrNiSn half-Heusler compounds by unidirectional solidification in short-duration μg.

2. Experimental

ZrNiSn was prepared by arc-melting from the constituent elements (Zr:Ni:Sn=1:1:1[mole]). The arc-melted sample was ground once, and the pellet made by this powder was annealed at 1273K in H_2 atmosphere. These pellets were set on the 2 different unidirectional solidification systems. In system (1), the sample directly contacts with the copper chill block; in system (2), the sample indirectly contacts with the copper plate through the quartz glass tube (**Fig.1**). The quartz glass tube was evacuated and filled with Ar gas up to a pressure of 0.1 MPa. The sample was heated in an infrared furnace at around 1673 K until it was completely melted. The sample was then unidirectionally solidified by contact with the copper block or plate. The μg experiments were perfomed using 10m drop tower at AIST and 2m drop tower at YNU. The obtained samples were analyzed by X-ray diffraction (XRD), optical microscopy (OM) and scanning electron microscopy (SEM).

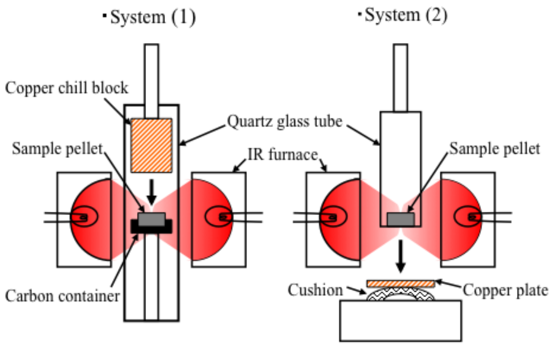

Fig.1 Schematic diagram of unidirectional solidification systems

3. Results and Discussion

Figure 2 shows that unidirectional solidified sample in normal gravity (1g) and μg by using system (1) and (2). Both solidified sample by using system (1) and (2) in 1g had no crystalline alignment. The solidified sample in μg by using system (1) had <111> crystalline alignment of ZrNiSn phase along the cooling direction, and that in μg by using system (2) had <100> crystalline alignment along the cooling direction. Because Microgravity conditions produce a motionless and forceless melt and the densest crystal plane in cubic system is [111], we obtaiend the sapmple with [111] orientation by using system (1). When the sample was solidified by using system (2), ZrO_2 layer was formed on the contact surface of the sample with quartz glass. The ZrO_2 layer in 1g sample showed random orientation, but that in μg sample showed {011} crystal planes. This orientaion of ZrO_2 layer was considered to be induced to prepare the μg sample with <100> crystalline alignment along the cooling direction.

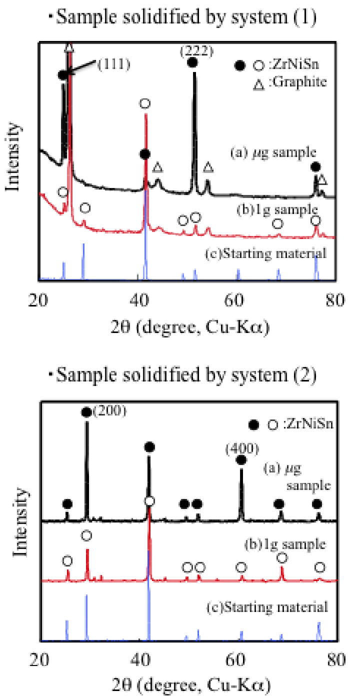

Fig.2 XRD result of the contact surface of the 1g and μg sample produced by different systems

References

1) T. Okutani, Y. Nakata and H. Nagai: Ann. N.Y. Acad. Sci., **1027** (2004) 158.
2) T. Okutani, H. Nagai, M. Mamiya, M. Shibuya and M. Castillo: Ann. N.Y. Acad. Sci., **1077** (2006) 146.

小惑星探査機「はやぶさ」の帰還と将来の太陽系探査

○山田哲哉 (宇宙航空研究開発機構)

Return of Asteroid Explorer Hayabusa and Future Solar System Exploration

Tetsuya YAMADA (Japan Aerospace Exploration Agency)

When future generations review the past human history, they will undoubtedly judge human exploration into space, with both machines and people, as one of its seminal developments. The present lecture relates the remarkable accomplishment in the field of the Japanese solar system exploration, the creation of the Japan Space Exploration Agency (JAXA) with the great achievement of the asteroid explorer Hayabusa. The lecture is extended to to the future plans in solar system exploration.

The asteroid explorer Hayabusa was launched by M-V rocket from Uchinoura Space Center, JAXA on May 9, 2003. The mission objectives are to explore the S-type asteroid Itokawa and to return its sample to the earth to contribute to the solar system science. Conquering several troubles encountered during totally 7 years of orbital flight, it returned to the earth and completed the powered-flight by the ion thrusters by the beginning of 2010. After successive trajectory correction maneuvers for the reentry, a small sample return capsule (SRC), separated from the mother spacecraft, has entered the earth atmosphere over the desert of the Australia on June 13, 2010, and landed successfully on the ground after passing through the excessively high aerodynamic heat load. The over 1,500 minor particles accommodated in the sampler container have proven to originate from the Itokawa. Thus, Japan has successfully returned the extra-terrestrial samples to the earth for the first time since the moon stone by the Apollo mission. Joint science team Hayabusa is eagerly investigating the Itokawa samples and is revealing the clue of beginning of our solar system.The lecture describes the overview of the innovative engineering technology of Hayabusa and is extended to the description how the troubles were conquered by splendid effort and cooperation among the project members.

Hayabusa 2 project has been authorized just now and the development works have started targeting launch in 2014. It is also an exciting mission searching for “the origin of life”, because one of the

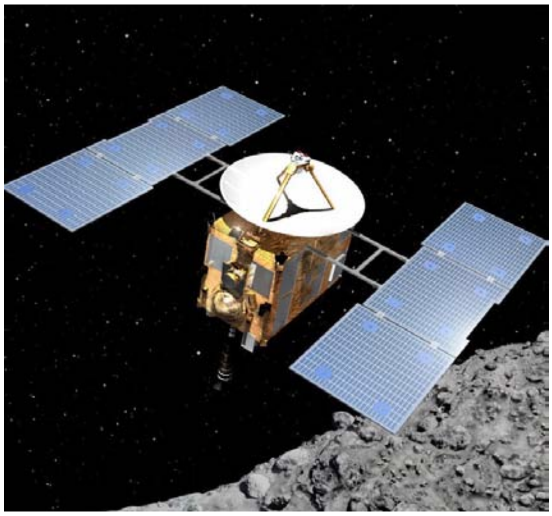

Asteroid Explorer Hayabusa;
launched on May 9th, 2003, and the sample return capsule was recovered on June 14-15, 2011.

objective is to return the sample from the C-type asteroid 1999JU3 including organic compounds. IKAROS (Interplanetary Kite-craft Accelerated by Radiation Of the Sun) was launched by H-IIA rocket on May 21, 2010. This is the world's first solar powered sail craft employing both photon propulsion and thin film solar power generation during its interplanetary cruise. Acceleration and navigation using the solar sail have then been demonstrated within the year. The technique is very promising to the solar exploration, because it saves propulsive energy: The second mission will take place in the late 2010’s. It will involve a large sized solar power sail with a diameter of 50 m, and will have integrated ion-propulsion engines. The destinations of the spacecraft will be Jupiter and the Trojan asteroids. Solar sail missions are also being studied in the United States and in European countries. Japan will lead future solar system exploration using robotic exploration (demonstrated by Hayabusa) and solar power sails.